An efficient timer and sizer of biomacromolecular motions

Justin Chan[1,2]¶, Hong-Rui Lin[1,¶], Kazuhiro Takemura[3,¶], Kai-Chun Chang[4], Yuan-Yu Chang[1], Yasumasa Joti[5], Akio Kitao[3] and Lee-Wei Yang [1,2,6*]*

1. Institute of Bioinformatics and Structural Biology, National Tsing Hua Univ., Taiwan
2. Bioinformatics Program, Taiwan International Graduate Program, Institute of Information Sciences, Academia Sinica, Taiwan
3. School of Life Science and Technology, Tokyo Institute of Technology, Japan
4. Institute of Molecular and Cellular Biology, National Taiwan University, Taiwan
5. XFEL Utilization Division, Japan Synchrotron Research Institute, Japan
6. Physics Division, National Center for Theoretical Sciences, Taiwan

¶Authors contributed equally to this work

*Corresponding authors:
Lee-Wei Yang
Tel: +88635742467;
Fax +88635715934;
Email: lwyang@life.nthu.edu.tw
Institute of Bioinformatics and Structural Biology, National Tsing Hua Univ.,
No. 101, Section 2, Kuang-Fu Road, Hsinchu 30013, Taiwan

Akio Kitao
Tel: +81-(0)3-5734-3373;
Fax: +81-(0)3-5734-3372;
Email: akitao@bio.titech.ac.jp
School of Life Science and Technology, Tokyo Institute of Technology,
M6-13, 2-12-1 Ookayama, Meguro, Tokyo 152-8550, JAPAN

Abstract

Life ticks as fast as how efficiently proteins perform their functional dynamics. Well-folded/structured biomacromolecules perform functions via large-scale intrinsic motions across multiple conformational states, which occur at timescales of nano- to milliseconds. Computationally expensive molecular dynamics (MD) simulation has been the only theoretical tool to gauge the time and sizes of these motions, though barely to their slowest ends. Here, we convert a computationally cheap elastic network model (ENM) into a molecular timer and sizer to gauge the slowest functional motions of proteins and ribosome. Quasi-harmonic analysis, fluctuation-profile matching (FPM) and the Wiener–Khintchine theorem (WKT) are used to define the "time-periods", *t*, for anharmonic principal components (PCs) which are validated by NMR order parameters. The PCs with their respective "time-periods" are mapped to the eigenvalues (λ_{ENM}) of the corresponding ENM modes. Thus, the power laws $t(\text{ns}) = 86.9\lambda_{ENM}^{-1.9}$ and $\sigma^2(\text{Å}^2) = 46.1\lambda_{ENM}^{-2.5}$ are established allowing the characterization of the time scales of NMR-resolved conformers, crystallographic anisotropic displacement parameters, and important ribosomal motions, as well as motional sizes of the latter.

TOC Graphics

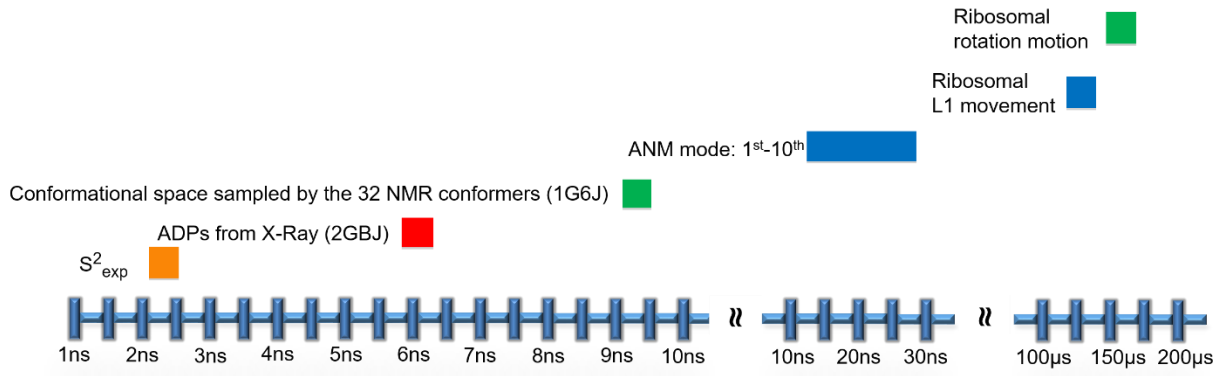

Keywords

protein dynamics, molecular dynamics simulations, principal component analysis (PCA), elastic network model (ENM), Wiener–Khintchine theorem, Einstein–Smoluchowski relation, time-correlation function, power spectrum, anharmonicity, order parameter, anisotropic displacement parameters, ribosome, ubiquitin

The magnitude of protein functional motions for folded proteins (or 'equilibrated' proteins) modulate the rates of their underlying physiological processes[1]. In principle, the wider the conformational spread is, the longer the time it takes, although the time and space relationship for protein motions damped in water may not be readily described by free diffusion of harmonic oscillators[2–7]. Understanding such a relation can bring important insights in protein dynamics including but not limited to the time scales of molecular controls as well as sizes of conformational changes that support the molecular function or facilitate two-body interactions. Molecular dynamics (MD) simulations, though computational costly, has been the only option to explore such a relationship[8–12], while larger and time-wise lengthier motions (> 10s of microseconds for large macromolecules) are still not within the reach of modern MD.

On the other hand, computationally cheap (>5 order cheaper than MD) elastic network models (ENMs) have been widely used for more than two decades[2–5] to study and predict the span (variance) of spatial distributions of protein conformations accessible to a molecule. These physically intuitive models have been used to study vibrational dynamics of all the proteins/supramolecules[6,7] in Protein Data Bank (PDB) where the "directions" of proteins' conformational changes as observed by x-ray crystallography have been satisfactorily reproduced in hundreds of applications and in database-wide studies[13,14] (see the caption in **Figure 1**). However, the absolute time scales and variances of functional modes cannot be directly assessed by ENM due to its harmonic approximation. Functional modes, particularly, involve motions at large scales, wherein proteins traverse across multiple intermediate states (corresponding to local traps in the energy landscape; see the left and middle in **Figure 1**), and therefore are anharmonic in nature[15–17]. In other words, the true challenge lies on how to properly define the "time periods" of these anharmonic modes, which cannot be simply inferred from the length of the simulation (a

small protein can travel several times on a given normal mode in a long MD simulation). Once defined, efficient and accurate methods are needed to predict the "*time periods*" and *absolute variances* of these anharmonic modes.

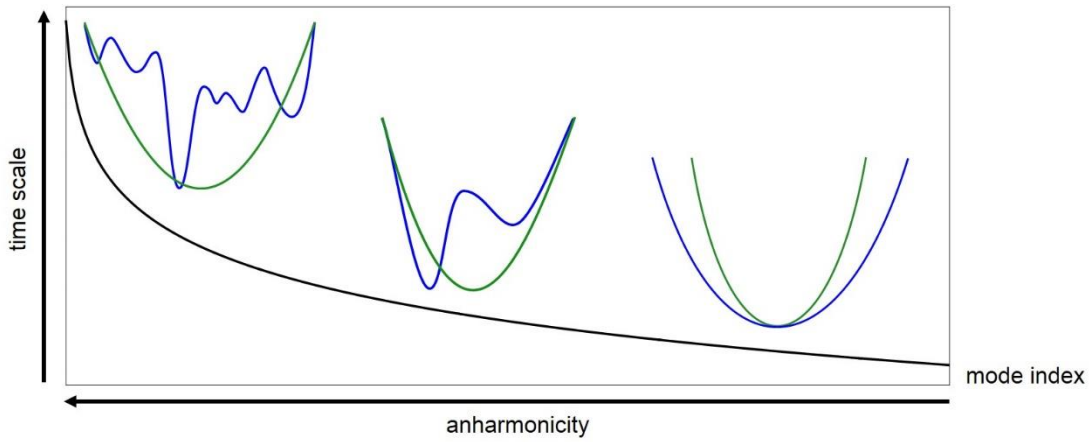

Figure 1. Time scales versus anharmonicity of the modes. The blue and green curves indicate the real and harmonically approximated energy landscapes, respectively. The slower the modes are, the larger the deviations from a simple harmonic approximation of the energy landscape (equivalently stated as having enriched anharmonicity[15–17]). ENM-approximated harmonic energy landscape forms an "envelope" that outlines the real anharmonic energy landscape[14] (to the left in **Figure 1**), which explains the observed correspondence between the theoretically predicted and experimentally characterized "directions" of conformational changes. However, the time scales and absolute spatial span of the modes, among the slowest and often functional, cannot be satisfactorily assessed given the harmonic approximation, which motivated us to design the current method to address the issue. The time scale estimated using the Intensity Weighted Period (IWP) method is introduced in this work (see below).

In this study, we first use Principal Component Analysis (PCA) of MD trajectories, time-correlation functions, Wiener–Khintchine theorem (WKT)[18] to define "time periods" for all the anharmonic and harmonic modes. Then, we use a mapping technique, Fluctuation Profile Matching (FPM), to map a dynamic variable (containing information of spatial spread of protein atoms; see below) or an ENM mode to a Principal Component (PC); hence the time scale of that PC can be assigned to the dynamic variable or ENM mode of interest. When every ENM mode is assigned a time scale or MD-sampled conformational spread (variance), we can then derive

corresponding power laws to describe how the time scale and conformational spread of a normal mode can be functions of its eigenvalue.

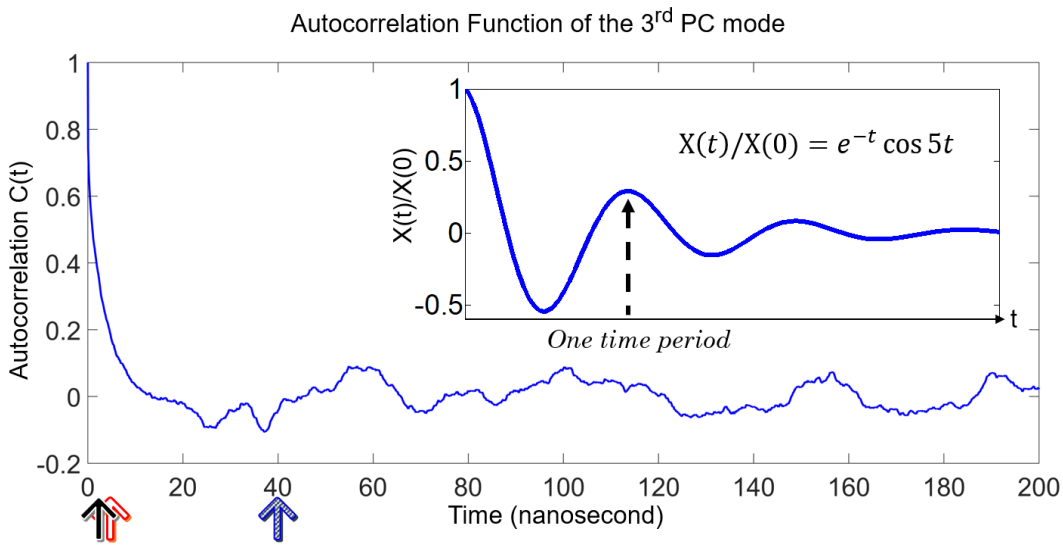

Figure 2. Defining the time scale of a PC mode using three methods. The profile of the autocorrelation function for the third PC mode, derived from PCA of a 600-ns simulation of ubiquitin (PDB ID: 1UBQ) and Wiener–Khintchine theorem (**eq 3**), is plotted. Three time constants τ_c = 2.34 ns (indicated by the black solid arrow), τ_r = 2.79 ns (red hollow arrow; obtained using fitting in the time domain) and τ_w = 40.45 ns (blue shaded arrow) that characterize the exponential decay of the autocorrelation function $C(t) = A\exp(-t/\tau_r)$, characteristic time such that $\tau_c = \sum_{i=1}^{M} C(t_i)\Delta t\,/C(0)$ and IWP of the power spectrum that is $\tau_w = 2\pi\sum_{i=1}^{M} S(\omega_i)\,\omega_i^{-1}/\sum_{j=1}^{M} S(\omega_j)$, respectively, are used to describe the vibrational relaxation process that mimics a damped harmonic oscillator. In addition, because the Fourier transform of an exponential function is a Lorentzian function[19], we can also obtain τ_r from fitting the entire power spectrum using a Lorentzian function. However, the resulting τ_r is much smaller than τ_c with a fitting correlation close to zero (data not shown). **(Inset)** Theoretical profile of one particle oscillating in an underdamped regime. The equation comparatively shows the equivalent decay and oscillation rate of the autocorrelation function. The vertical arrow indicates the time period, which in this illustrative example is 2π/5.

As a methodological overview in finer detail, **Figure 2** describes the autocorrelation function of a PC mode of ubiquitin. As previously described in either position[20] or velocity[15] autocorrelation functions, the function decays exponentially as a damped harmonic oscillator (**Figure 2**). We tried three methods to define the period, or "timescale" in this context, of this damped harmonic

oscillator for a PC mode. Among them, the Intensity Weighted Period (IWP; see definition below) requires the least assumption and appears to best describe the observed oscillatory behavior (**Figure 2**). Next, FPM identifies subsets of PCs that best reproduce (per the highest correlation) the experimentally observed profile of a given dynamical variable (including root-mean-square-fluctuations (RMSF) of a structural ensemble[21], anisotropic displacement parameters (ADPs)[22] and NMR order parameters[23]) and assign the IWP (or "time scale") of the slowest PC as the timescale of that profile. The subsets of PCs are generated by removing the top-*k* slowest PCs derived from long MD simulations. This is because we have previously[24] shown that deletion of the slowest ENM modes does not change the correlation between the predicted and experimentally observed B-factors, suggesting that dynamical profiles such as B-factors or anisotropic displacement parameters (ADP) do not include the protein's slowest motions given the confined crystalline environment[24]. In this study, we employ one of the most widely used ENMs, the anisotropic network model (ANM)[5,25,26]. Note that it was known that the mapping of PCA mode and ANM mode (or other ENM mode) is not a one-to-one relationship; a slow PC (ANM) mode is best interpreted by a few slowest ANM (PC) mode[27,28]. FPM provides a robust mapping between a PC mode *k* and an ANM mode *k'* (or an experimental variable) when the variance comprising all the PC modes higher than *k* has the highest correlation with the variance comprising all the ANM modes higher than *k'* (see **Supporting Information** for FPM's mathematical definition). The experimental variables here include NMR order parameters, ADPs from the X-ray structure and RMSF of NMR-solved structural ensemble of ubiquitin. To use the ANM as a convenient molecular timer and sizer, we match each ANM mode to a PC mode using FPM. Then, the timescale and variance of an ANM mode are assigned by the timescale and variance of the matched PC mode. We observe that the eigenvalues of ANM modes has a power law relationship with their

assigned timescales and variances. Applying the aforementioned procedure to three protein systems, ubiquitin, FGF2 and HP-NAP, we derive master equations for time and size of protein motions as power laws of ANM eigenvalues. We confirm the size power law by reproducing the observed ribosomal body rotation and estimate the time-scales for ribosomal body rotation and head swiveling motions to a narrower time range than those suggested by MD simulations and experiments.

Determining the time scales of the anharmonic modes

To estimate the true time scale of a PC mode, we first performed a 600-ns MD simulation for the 76 amino acid signaling protein, ubiquitin[29] (PDB ID: 1UBQ). PCA analysis[21] was carried out on the trajectory of the first 72 residues of ubiquitin, which are structurally ordered to derive the covariance matrix $<\Delta\mathbf{R}\Delta\mathbf{R}^{T}>$ and the projection of each snapshot to each of the eigenvectors (see details in the **Supporting Information**). In other words, a snapshot is a scalar value (PC mode coordinate) on the mode *k.*, $\mathbf{V}_k$. The total *M* snapshots projected on mode *k* together with padded *M* zeros result in a projection series $u_k(s) = \{u_{k0}, u_{k1}, \dots u_{kM-1}, 0^M, 0^{M+1} \dots 0^{2M-1}\}$, where u_{kj} means the *j*-th snapshot projected on the mode *k*, based on which the autocorrelation function for the mode *k* is calculated as follows. Let $\widetilde{u_k}(\omega) = \{\widetilde{u_{k0}}, \widetilde{u_{k1}}, \dots \widetilde{u_{k2M-1}}\}$ be the Fourier transform of $u_k(s)$, and the spectral density of the process $u_k(s)$ can be defined as $S_k(\omega) = \{|\widetilde{u_{k0}}|^2, |\widetilde{u_{k1}}|^2, \dots |\widetilde{u_{k2M-1}}|^2\}$. According to the Wiener–Khintchine theorem[18], the autocorrelation function of $u_k(s)$, $C_k(t)$, can be calculated as the inverse Fourier transform of the spectral density $S_k(\omega)$ such that

$$C_k(t) = < u_k(s)u_k(t+s) > = \frac{1}{2M}\sum_{f=0}^{2M-1} S_k(f)\, e^{\frac{2\pi i f t}{2M}} \tag{3}$$

where, $f = \omega/2\pi$ is the frequency. The mathematical details and computational implementation are provided in the **Supporting Information**.

Figure 2 shows that the $C_3(t)$ of the third PC mode, where $C_3(0)$ is unity (after normalization) at time zero, drops to where there are negative correlations and rises back above zero before eventually vanishing in an oscillatory manner. Most of the slowest modes demonstrate such a behavior, which can be approximated as a harmonic oscillator in underdamped regimes (illustrated in the inset of **Figure 2**). Our purpose here is to define a reasonable "time period" for such a process, which will be inferred as *the time scale (or "one period") of mode k*.

We initiated three attempts to define the time period of the PC mode. For the first one, we approximated the relaxation of $C(t)$ from unity to zero (the first time it hits a value barely larger than zero) as an exponential decay with a relaxation time constant of τ_r. Because the Fourier transform of an exponential function is a Lorentzian function[19], we can also obtain τ_r from fitting the entire power spectrum using a Lorentzian function, in contrast with fitting $C(t)$ within a limited time range [when $C(t) > 0$]. For the second method, we define the characteristic time constant τ_c, as the integration of $C(t)$ over the simulation time divided by $C(0)$ which is equal to τ_r if $C(t)$ is indeed an exponentially decaying function. For the third attempt, we simply take the intensity-weighted average of the periods in the power spectrum of $S(\omega)$ such that:

$$\tau_{w,k} = \frac{2\pi \sum_{i=1}^{M} S_k(\omega_i)\omega_i^{-1}}{\sum_{i=1}^{M} S_k(\omega_i)} \tag{4}$$

where $S_k(\omega_i)$ is the intensity (or "weight") for the frequency component ω_i (ω_i^{-1} is its corresponding period). As shown in **Figure 2**, τ_w, the intensity-weighted period (IWP), reaches a time scale where the $C(t)$ is close to the peak of the first wave, resembling a time period of a

damped oscillator, while neither relaxation time τ_r (obtained from the fitting in both time and frequency domains) nor characteristic time τ_c covers the time span for a period of an approximated damped oscillator.

Determining the time scales of experimentally observed dynamical variables

The spatial distribution of every residue (or every atom) in a protein near its folded (equilibrated) state can be observed by Cα RMSF of a NMR-resolved structural ensemble[21], NMR order parameters[23] and x-ray crystallographical anisotropic displacement parameters (ADPs)[22]. Plotting the dynamical value for each residue against its residue index results in so-called "observed fluctuation profiles" (oFPs) (**Figure 3, top,** black circles). Every residue has one magnitude of RMSF, one order parameter and 6 ADP values (including variance xx-, yy-, zz- and covariance xy-, yz- and xz- components[22]). Concurrently, we derive the theoretical counterparts of these measured variables from a MD snapshot-derived covariance matrix, $<\Delta\mathbf{R}\Delta\mathbf{R}^T>_{MD,k}$, comprising all the PC modes $\geq k^{th}$ mode (lower PC modes have larger variance)

$$< \Delta\mathbf{R}\Delta\mathbf{R}^{\boldsymbol{T}} >_{MD,k} = \sum_{a=k}^{3N-6} \lambda_a \mathbf{V}_a \mathbf{V}_a{}^{\boldsymbol{T}} \tag{5}$$

where $\mathbf{V}_a$ is the eigenvector with its corresponding eigenvalue, λ_a, taken from the diagonal of $\mathbf{\Lambda}$ in **eq 1** for the *a*'th PC mode; *N* is the total number of heavy atoms in the protein.

Next, we use FPM to find the *k* that can best reproduce the oFPs of interest, we seek the optimal k where the profile derived from $<\Delta\mathbf{R}\Delta\mathbf{R}^T>_{MD,k}$ has the best agreement with the oFPs by having the highest Pearson's correlation coefficient (σ_p)[30]. After finding the best *k* via fluctuation profile

matching (FPM), $\tau_{w,k}$ of the PC mode k is assigned to the observed dynamical variable, as its estimated time scale (see **Figure 3** and **Supporting Information** for examples).

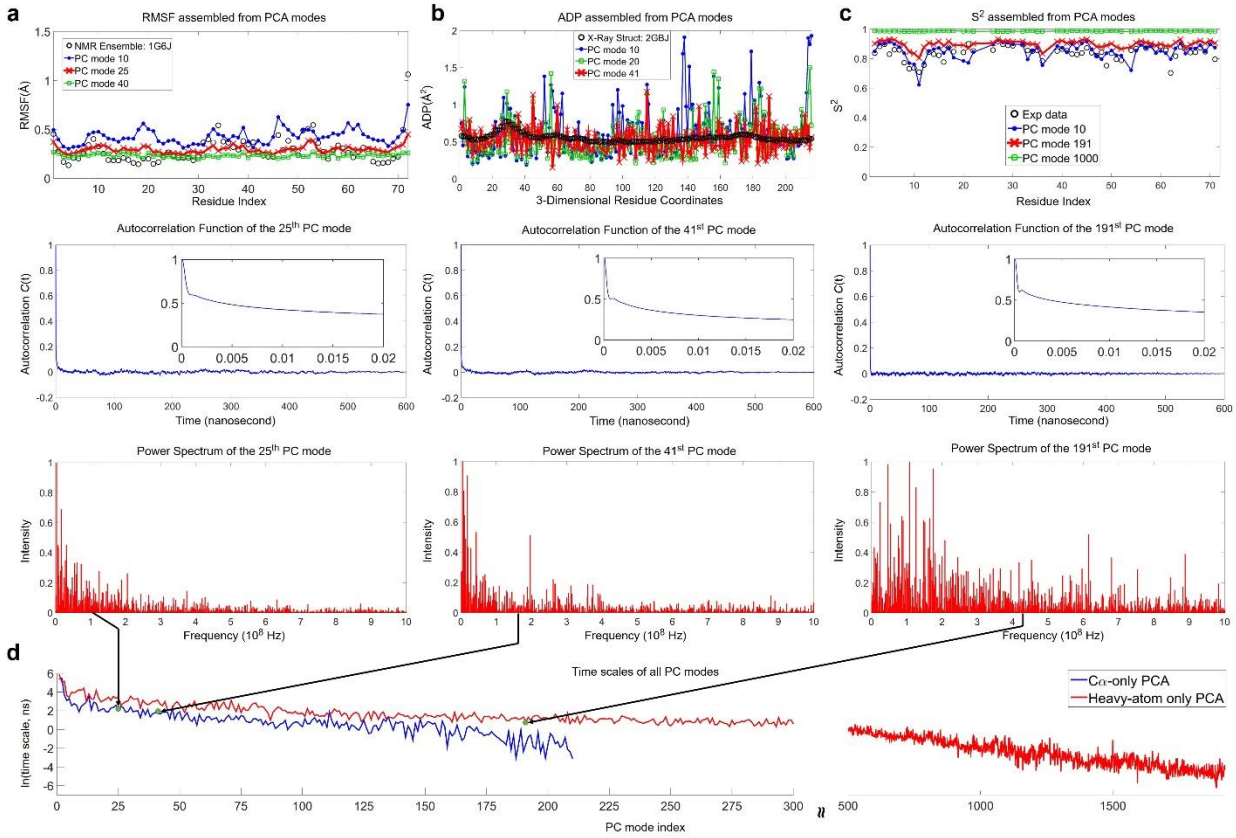

Figure 3. Time scale mapping for different experimental data that characterize protein dynamics. The first rows for **(a-c)** are, respectively, the oFP of RMSF derived from an NMR-determined ensemble (PDB: 1G6J), ADP values (only the diagonal elements are shown) and NMR-measured order parameters against residue index of ubiquitin, where the experimental profiles are plotted in scattered black circles, and the best fit PC mode profile is plotted in thick red lines. **(a, top)** The experimental profile best matches ($\sigma_p = 0.69$) the theoretical RMSF derived from a 600-ns MD simulation, where all PC modes ≥25 are included to contribute to $<\Delta\mathbf{R}\Delta\mathbf{R}^T>_{MD,k}$ (k = 25); further removing modes higher than mode 24 would impair the correlation. Profiles of different k values are also plotted for comparison. **(a, middle)** The autocorrelation function for the best-matched mode k = 25 is computed via WKT following **eq 3**. In addition, **(a, bottom)** its corresponding power spectrum, $S(\omega)$, plotted against its constituent frequencies $f = \omega/2\pi$, can be obtained before the inverse Fourier transform. Only the contributions of frequencies lower than 10^9 Hz are plotted. A black arrow is drawn to point from the implied IWP's frequency, ($1/\tau_w$), to its corresponding IWP (τ_w) in the ordinate (taken natural logarithm) of the chart in panel **(d)**. **(b and c)** In a similar spirit as **(a)**, panels **(b and c)** are plotted for the experimental ADPs (PDB: 2GBJ) and NMR order parameters[23] of ubiquitin, with the best matched modes determined as k=41 and k=191, respectively. Note that the PCAs performed for **(a and b)** are Cα-based and for **(c)**, the

PCA is based on all-heavy-atoms and H atoms bonded to backbone N's. **(d)** IWP (τ_w) is plotted against the PC mode index for both Cα-based ($3N - 6 = 210$ modes; in blue) and all-heavy-atom based ($3N - 6 = 1923$ modes; in red) PCA.

The NMR order parameters, S^2, describes the order of the backbone -NH bond vector $r_{ij} = (x_{ij}, y_{ij}, z_{ij})$ pointing from atom i to j (herein, i is N, and j is H) which can be approximated as[21,31,32]

$$S_{ij}^2 = \frac{3}{2}\begin{pmatrix} < x_{ij}^2 >^2 + < y_{ij}^2 >^2 + < z_{ij}^2 >^2 + \\ 2 < x_{ij}y_{ij} >^2 + 2 < x_{ij}z_{ij} >^2 + 2 < y_{ij}z_{ij} >^2 \end{pmatrix} - \frac{1}{2} \quad (6)$$

Here, the length of r_{ij} is normalized to unity. The angular brackets denote averages taken over the M snapshots; herein M = 6,000,000 or 1,200,000 are for the 600 ns and 120 ns trajectories, respectively. S^2 takes on values between 0, for freely rotated bonds (disordered), and unity, for perfectly "ordered" bonds. PCA is carried out for all the heavy atoms plus the hydrogen atoms in the amino (–NH) groups along the backbone of ubiquitin on the long 600-ns MD simulations and the associated five-constituent 120-ns sub-trajectories.

Through FPM, it was found that $\tau_{w,k=191}$ = 2.34 ns and $\sigma^2_{k=191}$ = 0.44 Å^2 (**Figure 3c** and see correlation as a function of PC mode index, peaked at the mode 191, in **Figure S2b**), characterizes the time scale and size of motion for the observed order parameter profiles[23]. When we applied the current method to shorter trajectories, it was found among five 120-ns simulations that the S^2_{exp} profile consistently maps to the PC modes with τ_w values between 0.7 ns and 1.0 ns (see one 120-ns result in **Figure S3a**).

Hence, despite different simulation lengths being used, our method consistently reports a time scale of 0.7 ns and 2.3 ns for this set of dynamics variables characterized by the NMR relaxation

experiments, consistent with the correlation time of methyl symmetry axis motion (300 to 500 ps)[33] using the extended model-free approach, while the "back-calculated" analysis of spectral densities using MD simulations reported time constants of 0.6, 0.9, and 1.5 ns[34].

Determination of time scales of the ENM modes and inference of time scales from the ENM eigenvalues

It is cumbersome to repetitively perform long MD simulations every time to characterize the time scales of experimentally observed dynamics variables. Here, we devised a computationally light molecular timer that can estimate the time scales of modes from anisotropic network model (ANM)[5,14]. To realize this, FPM of RMSF profiles derived from ANM modes and from MD PC modes was used to map each ANM mode to a PC mode. The ANM derived covariance matrix, $<\Delta\mathbf{R}\Delta\mathbf{R}^T>_{ANM,l}$, for all ANM modes $\geq l$ (lower ANM modes have lower frequencies or smaller eigenvalues) was calculated as follows

$$< \Delta\mathbf{R}\Delta\mathbf{R}^{\boldsymbol{T}} >_{ANM,l} = \frac{k_B T}{\gamma} \sum_{a=l+6}^{3N} \lambda_a^{-1} \mathbf{V}_a \mathbf{V}_a^{\boldsymbol{T}} \qquad (7)$$

where $\boldsymbol{V}_a$ and λ_a are the eigenvector and eigenvalue of the a'th ANM mode, respectively. While, γ is the universal spring constant, k_B is the Boltzmann constant and T is the absolute temperature with $\frac{k_B T}{\gamma}$ set to unity. The $\mathrm{RMSF}_{ANM,l}$ and $\mathrm{ADP}_{ANM,l}$ profiles were computed from the $<\Delta\mathbf{R}\Delta\mathbf{R}^{\boldsymbol{T}}>_{ANM,l}$ matrix with the same methods used for MD-derived profiles of RMSF and ADP.

FPM is applied to each ANM mode l's $\mathrm{RMSF}_{ANM,l}$ profile to identify the kth PC's $\mathrm{RMSF}_{MD,k}$ profile with the highest correlation. By doing this, every ANM mode l can be assigned the time scale (τ_w) of its best-matched k^{th} PC mode. If there are more than one ANM mode mapped to a PC

mode, the ANM mode having the highest correlation with that PC mode would be kept. We then fit the remaining ANM eigenvalues (λ_{ANM}) with their mapped time scales (t_{ANM}) in the form of a power law $t_{ANM} = c \times \lambda_{ANM}^{d}$ to obtain the constants c and d, as described in the **Supporting Information** and **Figure 4a**.

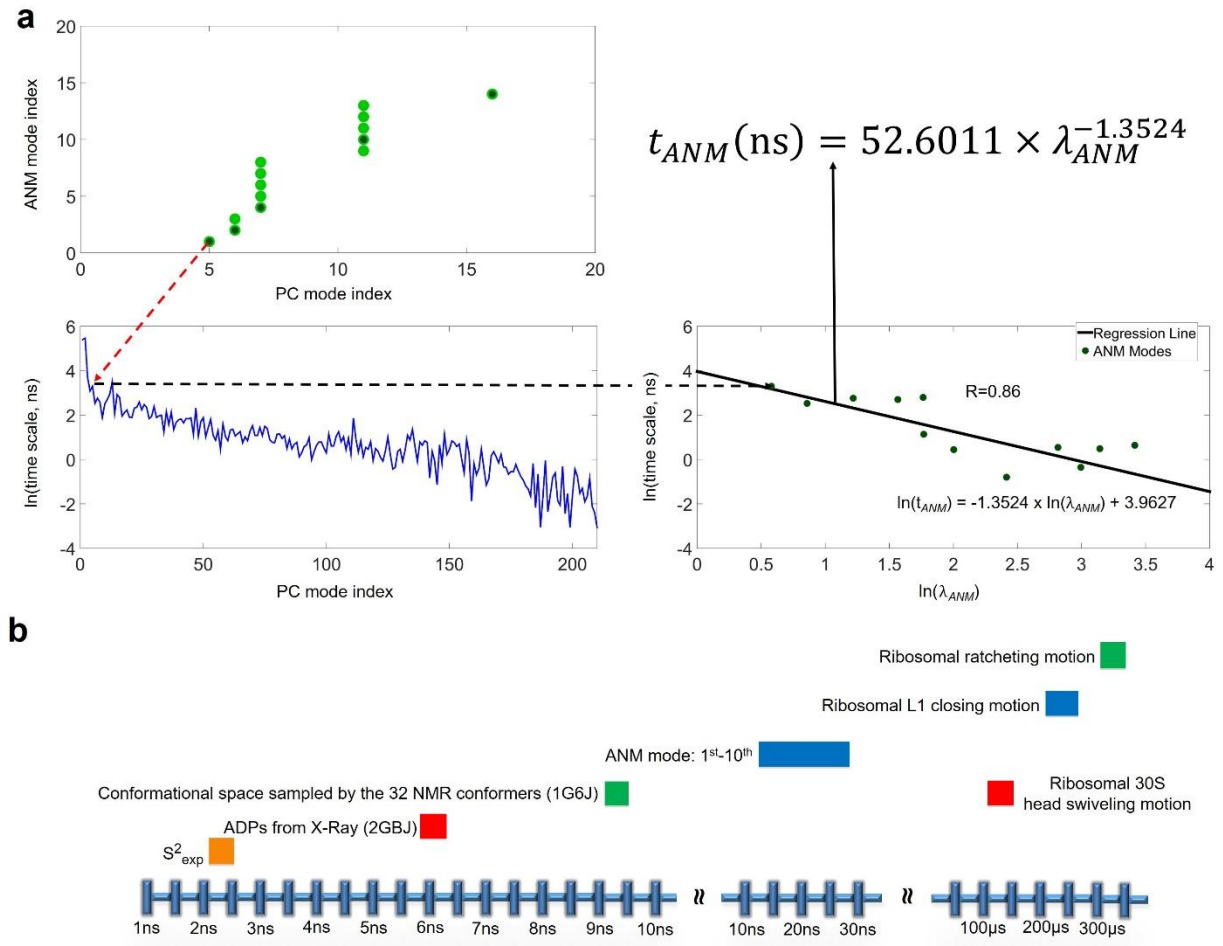

Figure 4. Frequency mapping for ANM to obtain the power law of τ_w as a function of ANM eigenvalues. (a) The ANM analysis and PCA of long MD trajectories are obtained for ubiquitin (residues 1-72, Cα-only). The τ_w of every PC mode obtained using IWP was mapped to the most correlated ANM mode using FPM. **(a, top left),** First l-1 ANM modes are removed to obtain a covariance matrix comprising modes $\geq l$. The RMSF of each residue, $\text{RMSF}_{ANM,l}$, is the square root of the sum of x-, y- and z-components of its variance. This $\text{RMSF}_{ANM,l}$ is compared to the $\text{RMSF}_{MD,k}$ comprising PC modes $\geq k$. Each ANM mode l (light-green circles) is mapped to the highest correlated PC mode k by comparing RMSF profiles. When multiple ANM modes are

mapped to the same PC mode k, only the pair with the highest correlation is kept (dark-green circles). The τ_w of the PC mode k is then assigned to the ANM mode l. For example, the first (l = 1) ANM mode maps to the 5th PC mode (red arrow). **(a, bottom left),** The τ_w's are plotted against the PC mode index (identical to the blue curve in **Figure 3d**). **(a, bottom right),** The τ_w's are plotted against λ_{ANM} (the eigenvalues of ANM modes). Linear regression gives the power law $t_{ANM}(\mathrm{ns}) = 52.6011 \times \lambda_{ANM}^{-1.3524}$ for ubiquitin. **(b)** Time scales of the examined dynamics variables, including the ANM modes, are assigned by the PCA+WKT+FPM approach for ubiquitin, except for the time scales of ribosomal motions that are estimated by the power law $t_{ANM}(\mathrm{ns}) = 65.4392 \times \lambda_{ANM}^{-2.1386}$ derived from the combined τ_w and λ_{ANM} of ubiquitin and FGF2.

For the case of ubiquitin, ANM mode 1 is mapped to PC mode 5 therefore it is assigned the time scale, $\tau_{w,k=5}$ = 27.03 ns (**Figure 4a**). Similarly, the RMSF_{ANM} for modes 4 and 10 are mapped to PC modes 7 and 11 with the corresponding time periods τ_w of 21.95 and 14.87 ns, respectively. This suggests that the motions described by the first 10 ANM modes for ubiquitin, or the slowest end of ANM, should occur within the timeframe of 13 to 28 ns (see **Figure 4b**). Fitting the λ_{ANM}'s with the t_{ANM}'s we obtain a power law for ubiquitin, $t_{ANM}(\mathrm{ns}) = 52.6011 \times \lambda_{ANM}^{-1.3524}$.

To extend the applicability of this method, we apply the aforementioned method to two other proteins. We performed PCA+IWP analysis on the 200-ns MD trajectories of an FGF2 monomer (126 residues; PDB ID: 1BFG) and HPNAP (144 residues; PDB ID: 1JI4) to derive time scales (τ_w) of each protein's PC modes. Then, we combined the mapped time scales of the ANM modes and the corresponding eigenvalues for these three proteins (ubiquitin, FGF2 and HPNAP) to derive the general power law $t_{ANM}(\mathrm{ns}) = 86.9387 \times \lambda_{ANM}^{-1.8886}$ (**Figure S4a**). We would like to acknowledge that the general power law derived here from the three proteins of different sizes (length; also see **Figure S4b**) is nowhere final and presented as a seminal effort for further studies and improvements.

In the **Supporting Information**, we provide a verification on how the time scales of several dynamics variables can be obtained using aforementioned general power law, as a function of ANM eigenvalue. Thus, a simple molecular timer that characterizes functional motions of biomolecules is obtained. **Figure 4b** summarizes the time scales of discussed experimental observables and ANM modes of interest.

Derive ANM power law for the sizes of functional motions

Since each ANM mode has been mapped to a PC mode, one can also describe the PC mode variance (the eigenvalue of PC mode) as a function of the corresponding ANM eigenvalue. Combining the aforementioned three protein cases, the linear regression of a log-log plot provides a new power law such that $\sigma^2(\text{Å}^2) = 46.0538 \times \lambda_{ANM}^{-2.5085}$ (see the **Supporting Information**). This power law, governing the sizes (variance) of motion as a function of ANM eigenvalues, together with the time power law jointly suggest that the protein's functional motions follow a $t^{1.33} \sim \langle \sigma^2 \rangle$ relationship. In the meanwhile, the normal mode theory provides a relation $\langle \sigma^2 \rangle = k_B T / m\omega^2$ for the harmonic oscillator (where ω is the frequency for the normal mode of interest), suggesting that $t^2 \sim \langle \sigma^2 \rangle$, while the Einstein–Smoluchowski relation (or fluctuation-dissipation theorem) for freely diffused particle in 1D describes a $\langle \sigma^2 \rangle = 2Dt$ relation, or equivalently $t \sim \langle \sigma^2 \rangle$. Our derived $t^{1.33} \sim \langle \sigma^2 \rangle$ relationship lies closer to free diffusion than to a harmonic oscillator.

Analysis of ribosomal motions

The power laws are applied to analyze the ribosomal body rotation motion (ratcheting)[6,35] between the 30S and 50S subunits of the *Thermus thermophilus* ribosome[35], which is essential for

ribosomal translocation during protein translation[36,37]. We perform ANM analysis on the non-rotated ribosome conformation and the 25th slowest ANM mode is identified as the ratcheting motion, see details in **Supporting Information**. We deform the ribosome by the size of mode 25 suggested by the variance power law and the rotated ribosome shows a 9° rotation which is close to the experimentally measured rotation of 7° (according to the non-rotated state [PDB ID: 4V6F] and rotated state [PDB ID: 4V9H])[38,39].

The estimated timescale of the ribosomal body-rotation (ratcheting) according to simulation[40] and stopped-flow[37,41] is between >1.3 μs and <5.0 ms, respectively. Individual power laws estimated from ubiquitin and FGF2 predicts the timescale to be between 11.5 μs and 651.9 μs, respectively. However, the HPNAP-derived power law estimates a timescale of less than 1.3 μs, inconsistent with the simulation results[40]. Therefore, for predicted time scales longer than 600 ns, which is the longest simulation we conducted to derive the previous power laws, we adopt the power law derived from ubiquitin and FGF2 only, which gives a $t_{ANM}(\mathrm{ns}) = 65.4392 \times \lambda_{ANM}^{-2.1386}$ (see **Figure S5**). With this power law, we obtain a timescale of 327.5 μs for the ribosomal ratcheting motion (see timescale estimates for all the slowest ribosomal normal modes in **Table S1**), which is just 1.8-fold longer than 180 μs, the time scale estimated by the power law derived from all the 3 proteins ($t_{ANM}(\mathrm{ns}) = 86.9387 \times \lambda_{ANM}^{-1.8886}$). Using the former power law (for estimated time scale > 600 ns), the L1 stalk closing and 30S head swiveling motion are estimated to have a time scale of 202-253 and 128 μs, respectively (see **Supporting Information)**.

To summarize, the two power laws we derived are combined to give $\langle\sigma^2\rangle = 0.1223t^{1.3282}$. Such a "guided" (structure-encoded) diffusion motion ($t \sim \langle\sigma^2\rangle^{0.75}$) is slower than a harmonic oscillator that travels with a ($t \sim \langle\sigma^2\rangle^{0.5}$)[5] relation, but faster than the free diffusion ($t \sim \langle\sigma^2\rangle$)[18]. The predicted time scale using our power law at 100s of microseconds to milliseconds is estimated to have an error of 2-4 fold or less than an order of magnitude. We hope that the introduced method to turn ENMs into a molecular timer and sizer can aid in our quantitative understanding of functional and anharmonic motions of biomolecules. The codes for performing the analysis are available on https://github.com/Hong-Rui/bioStructureM.

Methods

The details of all the methods of this study can be found in the **Supporting Information**.

Associated Content

Supporting Information. PDF file containing details of the principal component analysis (PCA), Wiener–Khintchine theorem (WKT), Intensity Weighted Period (IWP), Fluctuation Profile Mapping (FPM), theoretical profiles of RMSF, ADP and order parameters, Anisotropic Network Model (ANM), fitting the time and variance power laws and identification and prediction of the size and time scale of ANM modes corresponding to important ribosomal motions. Figures showing time scales computed using IWP, characteristic time and relaxation time, correlations between the MD derived RMSF, ADP and order parameter profiles using all PC modes $\geq k$ with their respective oFPs of Ubiquitin, computed order parameter from the 120 ns and 600 ns trajectories of Ubiquitin compared to the experimental order parameter, comparison of IWP with the power law estimated time scale, relationship between protein sizes and ANM's slowest mode and collectivity of the slowest 50 ANM modes of the non-rotated ribosome. Table containing the eigenvalues and time power law estimated time scales for the slowest 50 ANM modes of the non-rotated ribosome. 1UBQ.zip, FGF2.zip and HPNAP.zip: input files for performing MD simulations for Ubiquitin, FGF2 and HPNAP respectively.

Author Information

Notes

The authors declare no competing financial interests.

Acknowledgements

We acknowledge the computational resources supported by High Performance Computing Infrastructure (HPCI), Japan, by National Center for High-performance Computing (NCHC) of National Applied Research Laboratories (NARLabs) of Taiwan, and by supercomputers at the RCCS, The National Institute of Natural Science, and ISSP, The University of Tokyo. J.C.

acknowledges financial supports from MOST and Taiwan International Graduate Program, Academia Sinica, Taipei, Taiwan. This work is funded by the Ministry of Science and Technology (104-2113-M-007-019 and 106-2313-B-007-001-) and National Center for Theoretical Sciences, Taiwan to L.W.Y and by MEXT/JSPS KAKENHI (No. 25104002 and 15H04357) to A.K., as the "Priority Issue on Post-K Computer" (Building Innovative Drug Discovery Infrastructure Through Functional Control of Biomolecular Systems).

References

(1) Popovych, N.; Sun, S.; Ebright, R. H.; Kalodimos, C. G. Dynamically Driven Protein Allostery. *Nat. Struct. Mol. Biol.* **2006**, *13* (9), 831–838.

(2) Flory, P. J.; Gordon, M.; McCrum, N. G. Statistical Thermodynamics of Random Networks [and Discussion]. *Proc. R. Soc. A Math. Phys. Eng. Sci.* **1976**, *351* (1666), 351–380.

(3) Tirion, M. M. Large Amplitude Elastic Motions in Proteins from a Single-Parameter, Atomic Analysis. *Phys. Rev. Lett.* **1996**, *77* (9), 1905–1908.

(4) Bahar, I.; Atilgan, A. R.; Demirel, M. C.; Erman, B. Vibrational Dynamics of Folded Proteins: Significance of Slow and Fast Motions in Relation to Function and Stability. *Phys. Rev. Lett.* **1998**, *80* (12), 2733–2736.

(5) Atilgan, A. R.; Durell, S. R.; Jernigan, R. L.; Demirel, M. C.; Keskin, O.; Bahar, I. Anisotropy of Fluctuation Dynamics of Proteins with an Elastic Network Model. *Biophys. J.* **2001**, *80* (1), 505–515.

(6) Wang, Y.; Rader, A. J.; Bahar, I.; Jernigan, R. L. Global Ribosome Motions Revealed with Elastic Network Model. *J. Struct. Biol.* **2004**, *147* (3), 302–314.

(7) Li, H.; Chang, Y.-Y. Y.; Yang, L.-W. W.; Bahar, I. IGNM 2.0: The Gaussian Network Model Database for Biomolecular Structural Dynamics. *Nucleic Acids Res.* **2016**, *44* (D1), D415-22.

(8) Götz, A. W.; Williamson, M. J.; Xu, D.; Poole, D.; Le Grand, S.; Walker, R. C. Routine Microsecond Molecular Dynamics Simulations with AMBER on GPUs. 1. Generalized Born. *J. Chem. Theory Comput.* **2012**, *8* (5), 1542–1555.

(9) Shaw, D. E.; Maragakis, P.; Lindorff-Larsen, K.; Piana, S.; Dror, R. O.; Eastwood, M. P.; Bank, J. A.; Jumper, J. M.; Salmon, J. K.; Shan, Y.; et al. Atomic-Level Characterization of the Structural Dynamics of Proteins. *Science (80-.).* **2010**, *330* (6002), 341–346.

(10) Sanbonmatsu, K. Y.; Joseph, S.; Tung, C.-S. Simulating Movement of TRNA Into the Ribosome During Decoding. *Proc. Natl. Acad. Sci.* **2005**, *102* (44), 15854–15859.

(11) Ratje, A. H.; Loerke, J.; Mikolajka, A.; Brünner, M.; Hildebrand, P. W.; Starosta, A. L.; Dönhöfer, A.; Connell, S. R.; Fucini, P.; Mielke, T.; et al. Head Swivel on the Ribosome Facilitates Translocation by Means of Intra-Subunit TRNA Hybrid Sites. *Nature* **2010**, *468* (7324), 713–716.

(12) Whitford, P. C.; Onuchic, J. N.; Sanbonmatsu, K. Y. Connecting Energy Landscapes with Experimental Rates for Aminoacyl-TRNA Accommodation in the Ribosome. *J. Am. Chem. Soc.* **2010**, *132* (38), 13170–13171.

(13) Bahar, I.; Lezon, T. R.; Yang, L.-W.; Eyal, E. Global Dynamics of Proteins: Bridging between Structure and Function. *Annu. Rev. Biophys.* **2010**, *39* (39), 23–42.

(14) Li, H.; Chang, Y.-Y.; Lee, J. Y.; Bahar, I.; Yang, L.-W. DynOmics: Dynamics of Structural

Proteome and Beyond. *Nucleic Acids Res.* **2017**, *45* (W1), W374–W380.

(15) Kitao, A.; Hirata, F.; Gō, N. The Effects of Solvent on the Conformation and the Collective Motions of Protein: Normal Mode Analysis and Molecular Dynamics Simulations of Melittin in Water and in Vacuum. *Chem. Phys.* **1991**, *158* (2–3), 447–472.

(16) Kitao, A.; Go, N. Investigating Protein Dynamics in Collective Coordinate Space. *Curr. Opin. Struct. Biol.* **1999**, *9* (2), 164–169.

(17) Yang, L.-W.; Chng, C.-P. Coarse-Grained Models Reveal Functional Dynamics--I. Elastic Network Models--Theories, Comparisons and Perspectives. *Bioinform. Biol. Insights* **2008**, *2*, 25–45.

(18) McQuarrie, D. A. The Time-Correlation Function Formalism II. In *Statistical Mechanics*; University Science Books, 2000; pp 543–592.

(19) Boas, M. L. Mathematical Methods in the Physical Sciences. In *The Journal of Symbolic Logic*; 2006; Vol. 57, pp 340–389.

(20) Okan, O. B.; Atilgan, A. R.; Atilgan, C. Nanosecond Motions in Proteins Impose Bounds on the Timescale Distributions of Local Dynamics. *Biophys. J.* **2009**, *97* (7), 2080–2088.

(21) Yang, L.-W.; Eyal, E.; Bahar, I.; Kitao, A. Principal Component Analysis of Native Ensembles of Biomolecular Structures (PCA_NEST): Insights into Functional Dynamics. *Bioinformatics* **2009**, *25* (5), 606–614.

(22) Eyal, E.; Chennubhotla, C.; Yang, L.-W.; Bahar, I. Anisotropic Fluctuations of Amino Acids in Protein Structures: Insights from X-Ray Crystallography and Elastic Network Models. *Bioinformatics* **2007**, *23* (13), i175–i184.

(23) Tjandra, N.; Feller, S. E.; Pastor, R. W.; Bax, A. Rotational Diffusion Anisotropy of Human Ubiquitin from 15N NMR Relaxation. *J. Am. Chem. Soc.* **1995**, *117* (50), 12562–12566.

(24) Yang, L.-W.; Eyal, E.; Chennubhotla, C.; Jee, J.; Gronenborn, A. M.; Bahar, I. Insights into Equilibrium Dynamics of Proteins from Comparison of NMR and X-Ray Data with Computational Predictions. *Structure* **2007**, *15* (6), 741–749.

(25) Chandrasekaran, A.; Chan, J.; Lim, C.; Yang, L.-W. Protein Dynamics and Contact Topology Reveal Protein-DNA Binding Orientation. *J. Chem. Theory Comput.* **2016**, *12* (11), acs.jctc.6b00688.

(26) Li, H.; Sakuraba, S.; Chandrasekaran, A.; Yang, L.-W. Molecular Binding Sites Are Located near the Interface of Intrinsic Dynamics Domains (IDDs). *J. Chem. Inf. Model.* **2014**, *54* (8), 2275–2285.

(27) Nicolay, S.; Sanejouand, Y.-H. Functional Modes of Proteins Are among the Most Robust. *Phys. Rev. Lett.* **2006**, *96* (7), 078104.

(28) Bakan, A.; Bahar, I. The Intrinsic Dynamics of Enzymes Plays a Dominant Role in Determining the Structural Changes Induced upon Inhibitor Binding. *Proc. Natl. Acad. Sci.*

2009, *106* (34), 14349–14354.

(29) Vijay-kumar, S.; Bugg, C. E.; Cook, W. J. Structure of Ubiquitin Refined at 1.8 Å Resolution. *J. Mol. Biol.* **1987**, *194* (3), 531–544.

(30) Pearson, K. Note on Regression and Inheritance in the Case of Two Parents. *Proc. R. Soc. London* **1895**, *58* (1), 240–242.

(31) Henry, E. R.; Szabo, A. Influence of Vibrational Motion on Solid State Line Shapes and NMR Relaxation. *J. Chem. Phys.* **1985**, *82* (11), 4753.

(32) Best, R. B.; Vendruscolo, M. Determination of Protein Structures Consistent with NMR Order Parameters. *J. Am. Chem. Soc.* **2004**, *126* (26), 8090–8091.

(33) Lee, A. L.; Flynn, P. F.; Wand, A. J. Comparison of 2 H and 13 C NMR Relaxation Techniques for the Study of Protein Methyl Group Dynamics in Solution. *J. Am. Chem. Soc.* **1999**, *121* (12), 2891–2902.

(34) Nederveen, A. J.; Bonvin, A. M. J. J. NMR Relaxation and Internal Dynamics of Ubiquitin from a 0.2 Ms MD Simulation. *J. Chem. Theory Comput.* **2005**, *1* (3), 363–374.

(35) Tama, F.; Valle, M.; Frank, J.; Brooks, C. L. Dynamic Reorganization of the Functionally Active Ribosome Explored by Normal Mode Analysis and Cryo-Electron Microscopy. *Proc. Natl. Acad. Sci.* **2003**, *100* (16), 9319–9323.

(36) Frank, J.; Agrawal, R. K. A Ratchet-like Inter-Subunit Reorganization of the Ribosome during Translocation. *Nature* **2000**, *406* (6793), 318–322.

(37) Cornish, P. V.; Ermolenko, D. N.; Noller, H. F.; Ha, T. Spontaneous Intersubunit Rotation in Single Ribosomes. *Mol. Cell* **2008**, *30* (5), 578–588.

(38) Jenner, L. B.; Demeshkina, N.; Yusupova, G.; Yusupov, M. Structural Aspects of Messenger RNA Reading Frame Maintenance by the Ribosome. *Nat. Struct. Mol. Biol.* **2010**, *17* (5), 555–560.

(39) Tourigny, D. S.; Fernandez, I. S.; Kelley, A. C.; Ramakrishnan, V. Elongation Factor G Bound to the Ribosome in an Intermediate State of Translocation. *Science (80-.).* **2013**, *340* (6140), 1235490–1235490.

(40) Whitford, P. C.; Blanchard, S. C.; Cate, J. H. D.; Sanbonmatsu, K. Y. Connecting the Kinetics and Energy Landscape of TRNA Translocation on the Ribosome. *PLoS Comput. Biol.* **2013**, *9* (3), e1003003.

(41) Guo, Z.; Noller, H. F. Rotation of the Head of the 30S Ribosomal Subunit During MRNA Translocation. *Proc. Natl. Acad. Sci.* **2012**, *109* (50), 20391–20394.